



**Journal of  
Mechanics of  
Materials and Structures**

**A NOVEL APPLICATION OF A LASER DOPPLER VIBROMETER  
IN A HEALTH MONITORING SYSTEM**

Davood Rezaei and Farid Taheri

**Volume 5, No. 2**

**February 2010**

 **mathematical sciences publishers**

## A NOVEL APPLICATION OF A LASER DOPPLER VIBROMETER IN A HEALTH MONITORING SYSTEM

DAVOOD REZAEI AND FARID TAHERI

This paper presents the results of an experimental study of the applicability of the laser Doppler vibrometer (LDV) as a potential measurement tool for structural health monitoring in pipelines. In this case, use of the LDV has been integrated into a novel damage detection method referred to as the empirical mode decomposition (EMD) energy damage index. This method involves monitoring the free vibrations of a pipe through sensors, followed by decomposition of the sensor generated signals using EMD, and subsequently comparing an energy term of the pipe in its healthy state to that of the same pipe in a damaged state. In the experiment, a single beam LDV was utilized to acquire the vibration of a cantilever steel pipe impacted by an impulse hammer. Three cases were studied: pipes with a single half-circumferential damage, a single full-circumferential damage, and with multiple circumferential damages. The integrity of the LDV results was verified by comparison with those obtained from piezoceramic sensors bonded to the pipe surface. The results confirmed the effectiveness of the LDV and its integration into the proposed EMD damage index for identifying and locating single and multiple damages. Compared to piezoceramic sensors, the LDV, as a remote and accurate optical measurement system, provided more satisfactory identification of single and multiple damages and can therefore be successfully utilized in structural health monitoring.

### Introduction

Despite the development of new sources of energy, the world economy is still heavily dependent upon petroleum, which is distributed in the form of oil and natural gas to numerous industries through widespread pipeline networks. Consequently, pipelines should always be maintained in a healthy condition to ensure the safe, reliable, and effective transportation of petroleum and other chemicals. Cracking and corrosion are the most common sources of damage in an operative pipeline, and may interrupt energy supplies and result in severe property damages and/or industry shut downs. These damages ultimately result in large repair, environmental clean-up, and legal costs. To avoid such misfortunes, the use of different structural health monitoring (SHM) methodologies is becoming increasingly common. The main purpose of SHM is to increase operational reliability and effectiveness via pipeline monitoring by detecting damage at its earliest stage and thereby reducing the risk of interruption of the energy supply.

In addition to common nondestructive damage detection methods in pipelines (visual inspection, X-ray, magnetic particle, and ultrasonic), modal based damage identification methods have been considered by many researchers. In these methods, deviations in specific dynamic characteristics of the structure before

---

*Keywords:* structural health monitoring, vibration-based damage detection, laser Doppler vibrometer, pipeline damage detection, piezoceramic sensors, empirical mode decomposition.

The financial support of the Natural Sciences and Engineering Council of Canada (NSERC) in support of this work is gratefully acknowledged.

and after damage are treated as the measures for damage identification. Every modal based SHM requires two key elements: sensors, which monitor the structural vibrations, and a method of data interpretation for extraction of the damage sensitive features.

Accelerometers and piezoelectric sensors (PZTs) are two well-known sensors used for capturing vibration in various applications such as mechanical systems, buildings, bridges, and aircrafts. Accelerometers have been commonly used to measure real-time acceleration of structures caused by vibration [Peeters et al. 2001; Hong et al. 2002; Kim and Melhem 2004; Lin et al. 2005]. There is also extensive work in the literature which considers the use of PZTs to monitor vibration [Banks et al. 1996; Jian et al. 1997; Soh et al. 2000; Winston et al. 2001; Fukunaga et al. 2002; Giurgiutiu et al. 2002]. Among conventional sensors in SHM, PZTs have the advantages of being small, light, inexpensive, and self-excited with the further benefits of having a high signal to noise ratios and being easily integrated into structures.

Despite the advantages of conventional contact sensors, such as accelerometers and PZTs, they still must be attached to the monitored structure. The necessity of direct contact with the structure introduces several drawbacks: added mass in the system (especially in the case of accelerometers on lightweight components), sensor slippage, sensor damage, failure in harsh environments, and the considerable difficulty of setting a large number of sensors on a structure and wiring them to a data acquisition system. Furthermore, most conventional sensors cannot cover the high frequency domain because of low measurement accuracy and inadequate sensitivity.

Greater sensitivity is required to pick up the minuscule amplitudes usually observed in structures undergoing vibration [Kaito et al. 2005]. There are also cases where access to the components is difficult. In order to overcome these shortcomings, important innovations have been achieved in the field of noncontact sensors by introducing laser-based measurements. Among the different laser-based methods, the laser Doppler vibrometer (LDV) is one of the most common techniques. For more information on laser Doppler vibrometry, the reader is referred to [Polytec 2009]. As a replacement for traditional sensors, LDVs are widely used for vibration measurements in fields such as biomedicine and field measurements such as quality control testing, material characterization, casting systems, structural testing, and damage detection in aerospace as well as civil and mechanical engineering. LDVs are able to monitor vibrations with a high degree of accuracy, sensitivity, and resolution. An LDV monitors the velocity and displacement of a vibrating object through the frequency shift between the laser beam projecting to the object and the reflected beam.

Kaito et al. [2005] employed an LDV scanning system to measure the vibration of real-scale structures such as steel girders and reinforced concrete decks of actual bridges. For the steel members, this study verified that the LDV and the accelerometer results matched with a high degree of accuracy in the time and frequency domains. It was reported that the accuracy of the LDV was reduced due to low laser reflection when the specimen was a concrete or dirt-adhering steel member. To overcome this problem, Kaito et al. [2005] suggested that a surface treatment, such as reflective tape, should be applied prior to measuring.

A comparative study performed by Nassif et al. [2005] showed that an LDV, as a noncontact and nondestructive measuring system, could provide accurate results for monitoring bridge vibration and deflection. Moreover, the LDV's results compared well with results from contact sensors such as linear variable differential transformers (LVDTs) mounted on the structure. This study also proved the capabilities of an LDV in interpreting accurate velocity measurements compared with mounted geophone



sensors. Therefore, an LDV can replace two systems (LVDT and geophone) for measuring vibration deflection and velocity while maintaining sufficient accuracy.

[Khan et al. \[2000\]](#) performed a set of experiments to detect cracks in structures with a scanning laser Doppler vibrometer (SLDV). Their study focused on detecting cracks in a cantilever beam, a concrete beam, and plates. They found that if the defects are such that they produce localized mode-shape discontinuities, the SLDV can successfully detect and locate damages. [Khan et al. \[2000\]](#) also reported that speckle noise could affect the results which led them to recommend using a low-pass filter to improve measurement quality.

As mentioned previously, the analysis and interpretation of a structure's dynamic response is a key factor in an effective and successful damage identification technique. There is a vast amount of work in the published literature utilizing different modal properties as damage sensitive features such as natural frequencies and mode shapes [[Peeters et al. 1996](#); [Hassiotis 2000](#); [Wang et al. 2001](#); [Kim et al. 2003](#); [Kim and Chun 2004](#)], modal strain energy [[Shi et al. 2000](#)], and stiffness matrices [[Ren and De Roeck 2002](#); [Hwang and Kim 2004](#)]. Other researchers have focused on vibration signal processing and have introduced methods based on frequency domain techniques, such as the Fourier transform, or based on time-frequency domain decompositions, such as the wavelet transform method [[Douka et al. 2004](#); [Kim and Melhem 2004](#); [Ovanesova and Suarez 2004](#); [Cheraghi et al. 2005b](#)]. An emerging signal time-frequency processing technique called the Hilbert–Huang transform (HHT) has recently been investigated in the field of SHM and has proven its potential in damage detection [[Xu and Chen 2004](#); [Cheraghi et al. 2005a](#); [Lin et al. 2005](#); [Liu et al. 2006](#); [Cheraghi and Taheri 2007](#); [2008](#)]. This method employs a decomposition technique called empirical mode decomposition (EMD), which is used to decompose the signal into basic oscillatory modes that contain crucial information about the structure's dynamic characteristics and from which damage sensitive features can be deduced. These oscillatory modes are referred to as intrinsic mode functions (IMFs).

[Xu and Chen \[2004\]](#) experimentally investigated the applicability of EMD for identifying the damage resulting from stiffness changes in a three-story shear building model. The structure was monitored continuously under free vibration, random vibration, and earthquake simulation. [Xu and Chen \[2004\]](#) were successful in identifying the damage time instant and damage location through spikes in the IMF derived from the EMD.

[Lin et al. \[2005\]](#) employed the HHT technique to identify damage in an IASC-ASCE benchmark four-story building under ambient vibration. In this study, the damage was identified by a comparison of the structural stiffness and damping, obtained by the HHT technique, between the intact and damaged structure.

[Liu et al. \[2006\]](#) experimentally investigated the applicability of the HHT technique for damage detection in the benchmark problem (a four-story building), developed by the University of British Columbia. They could identify the damage and instant of occurrence of damage, based on a comparison of the first three IMFs and their time-frequencies between the undamaged and damaged structure. The damaged structure was simulated by removing bracings and loosening bolts.

In [[Cheraghi et al. 2005a](#); [Cheraghi and Taheri 2007](#); [2008](#)] an SHM methodology was introduced based on the HHT and developed a novel damage index, called the EMD energy damage index (DI), which uses the energy of the first IMF of a structure's response signals in the healthy and damaged states. This method was theoretically applied to a 6-DOF mechanical system [[Cheraghi and Taheri 2008](#)] and

successfully detected the damage. The integrity of the proposed DI was also verified experimentally [Cheraghi et al. 2005a] to detect the unbounded region in an adhesively bonded joint in PVC pipes. For further verification of the EMD energy DI, Cheraghi and Taheri [2007] carried out a numerical study to detect damage in a cantilever aluminum pipe having various forms of defects simulated by removing material from the pipe surface at different locations. They applied the Fourier transform, Wavelet transform, and EMD energy DI methods; it was concluded that the EMD and wavelet approaches were the most successful methods in detecting the locations and the EMD was the best method for identifying damage severity.

In the present work, a set of experiments was completed to further investigate the applicability of the EMD energy DI introduced in [Cheraghi and Taheri 2008]. The experiments included a cantilever steel pipe having different damage cases in terms of defect location, number, and severity. The damages were created to simulate corrosion; they were created by manually grinding the pipe to remove material from its surface. The pipe was excited using an impulse hammer and the free vibrations generated were captured via an LDV. MATLAB code was written to perform the signal processing including data filtration and cleansing, decomposition of the signals via EMD, and calculation of the EMD energy. To verify the performance of the LDV, its results were compared with those obtained from piezoceramic sensors bonded to the pipe surface. The capability of both the LDV and PZTs for the extraction of the pipe's natural frequencies has been investigated. The results of the proposed damage detection methodology with the integrated LDV are presented, discussed and compared with those obtained from the PZTs.

### EMD energy damage index

Huang et al. [1998] introduced the Hilbert–Huang transform (HHT) signal processing method, which almost satisfied all the requirements for processing linear, nonlinear, stationary, and nonstationary signals. The HHT consists of two main parts: the EMD and the Hilbert transform. The EMD method decomposes a real signal into a collection of simpler modes or intrinsic mode functions (IMFs) which are basically associated with energy at different time scales and contain important data characteristics [Huang et al. 1998]. The Hilbert transform, once applied to IMFs, produces an energy-frequency-time distribution of the data known as a Hilbert spectrum. In general, the decomposition resulting from an HHT is well localized in the time-frequency domain and reveals important information within its data.

The procedure of sifting is schematically illustrated in Figure 1. To extract the IMFs for a given time signal  $x(t)$ , two cubic splines are fitted through the local maxima and minima to produce the upper and lower envelopes of the original signal, respectively (note that the upper and lower envelopes should contain all the data). Then the mean,  $m_1(t)$ , of these two splines is calculated and subtracted from the original signal. The difference between the signal and mean,  $h_1(t)$ , is called the first component, defined as  $h_1(t) = x(t) - m_1(t)$ .

Now  $h_1$  is treated as the original time signal and the sifting process is repeated to get the next component (that is,  $h_{11}(t) = h_1(t) - m_{11}(t)$ ). Each step of the sifting process produces a more symmetric signal with respect to the zero mean. To achieve the desired symmetry, more siftings have to be performed, mathematically represented by  $h_{1k}(t) = h_{1(k-1)}(t) - m_{1k}(t)$ .

If the sifting process continues to the extreme, it will remove the physically meaningful amplitudes and fluctuations. In response, Huang et al. [1998] proposed a criterion for limiting the size of the standard

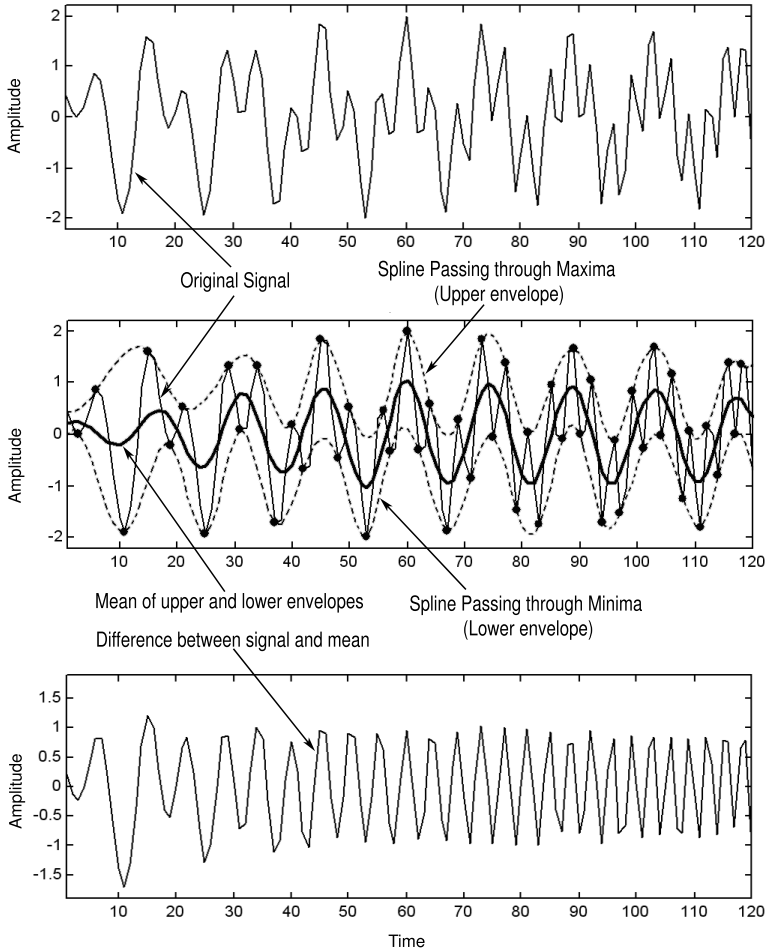


**Figure 1.** Schematic of the EMD sifting process.

deviation (SD) computed from two successive sifting results. This stoppage criterion is expressed as

$$SD = \sum_{t=0}^T \left[ \frac{|h_{1(k-1)}(t) - h_{1k}(t)|^2}{h_{1(k-1)}^2(t)} \right]. \tag{1}$$

If the SD is smaller than a predetermined value (usually between 0.2 and 0.3), the sifting process is stopped and  $h_{1k}(t)$  is called the first IMF component ( $c_1(t)$ ) of the signal; that is  $c_1(t) = h_{1k}(t)$ .

The first IMF component  $c_1(t)$  contains the finest scale or the shortest period component of the signal. Each IMF satisfies two conditions. Firstly, the numbers of extrema and zero crossings either are equal or differ by one. Secondly, the average of the envelopes, defined by the local maxima and local minima, is zero. To derive the other IMFs,  $c_1(t)$  is removed from the signal:  $r_1(t) = x(t) - c_1(t)$ .

The residue  $r_1(t)$  contains the larger scales or longer period components. Then  $r_1(t)$  is considered as the new signal and the sifting process is performed on it to obtain the second IMF component. This procedure is repeated for all subsequent  $r_i(t)$  to derive the longer period components. At each repetition, the signal is modified with respect to the obtained IMF:  $r_n(t) = r_{n-1}(t) - c_n(t)$ .

After extracting all the IMFs, the original signal is decomposed into  $n$  empirical modes and a residue  $r_n(t)$ , which can be either the mean trend or a constant. Hence,

$$x(t) = \sum_{i=1}^n c_i(t) + r_n(t). \quad (2)$$

In the present work, the damage index (DI) introduced by [Cheraghi and Taheri \[2008\]](#) was used to identify and locate damage in a cantilever steel pipe. This DI is based on the energy of the vibration signal's first IMF. According to this method, the dynamic characteristics of the healthy structure during free vibration are collected through sensors; the acquired signals are then passed through a band-pass filter to ensure the existence of the first natural frequency within the data. This is followed by extraction of the first IMF through EMD as described in the previous paragraphs. Finally, the energy of the first IMF for each sensor is established by:

$$E = \int_0^{t_0} (c_1(t))^2 dt, \quad (3)$$

where  $c_1(t)$  is the first IMF,  $t_0$  is the duration of the signal, and  $E$  is a scalar value representing the energy of the first IMF. As mentioned earlier, the first IMF contains the highest frequency component within the signal. Furthermore, structural damage is associated with higher frequencies and therefore only the first IMF is considered in the proposed DI.

The above procedure is repeated for the same structure in its damaged state to determine the energy of each sensor's first IMF. The last step is the application of the EMD energy DI to each sensor:

$$DI = \left| \frac{E_{\text{Healthy}} - E_{\text{Damaged}}}{E_{\text{Healthy}}} \right| \times 100. \quad (4)$$

Once the DI is calculated for each sensor (for each measurement location when using a single LDV), the existence and locations of damages may be determined by associating high index values with the existence of damage close to the respective sensors.

### Experimental setup

The test specimen used in this study was an API compliant [\[API 2000\]](#) standard steel pipe commonly used in oil and gas pipelines. The pipe was size  $6^{5/8}$ , grade A; its specifications are listed in [Table 1](#). [Figure 2](#) is an image of the experimental setup showing the pipe as a cantilever supported by two clamps at one end. The clamps are bolted to a massive structure in order to provide a rigid support and to reduce vibration dissipation through support flexibility.

A VibroMet 500 single beam LDV, manufactured by MetroLaser, Inc., is used in this study. The VibroMet 500 consists of a laser head and an electronic controller box. The laser head contains a diode

| Pipe size $6^{5/8}$ , Grade A, API Standard |          |     |                        |
|---|----------|-----|------------------------|
| Outside diameter                            | 168.3 mm | $E$ | 200 GPa                |
| Wall thickness                              | 6.4 mm   | $n$ | 0.30                   |
| Length                                      | 2.0 m    | $r$ | 7850 kg/m <sup>3</sup> |

**Table 1.** Dimensions and properties of the pipe.

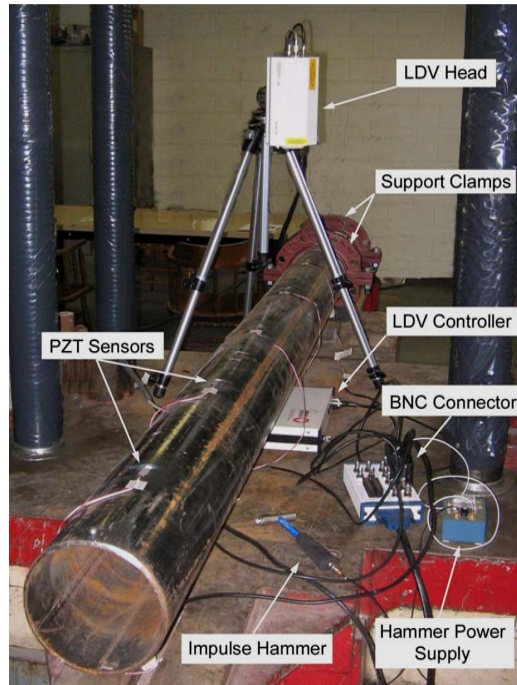


**Figure 2.** Experimental setup of the cantilever steel pipe and data acquisition equipment.

laser, a Bragg cell, a photodetector, and front-end electronics. The electronic controller contains the power supply, RF power for the Bragg cell, and an analog demodulator, which processes the laser head output and provides an analog velocity signal of the vibrations in real time. The electronic controller also contains a signal strength indicator, two selectable velocity ranges, and five selectable low pass filters (1, 2, 5, 10, and 20 kHz) which may be used to improve the signal to noise ratio of certain spectral bands.

As mentioned before, in order to compare and verify the results obtained from the LDV, the dynamic response of the pipe was monitored by PZTs bonded to the upper surface of the pipe (see Figure 2). The sensors were of type PZT-5H available in  $72.4 \times 72.4$  mm sheets from Piezo Systems, Inc. The PZT sensors were cut into small pieces ( $24 \times 10$  mm) and then bonded to the pipe surface using Araldite 2011 two part epoxy, distributed by Huntsman Advanced Materials Americas, Inc. These sensors are polarized through the thickness, so two electrodes were soldered to the top and bottom surfaces of each sensor.

In order to attain a good description of pipe vibration, five locations along the pipe were selected for LDV measurement. Because of the dark surface of the pipe, which is a poor reflector for the laser beam, a white spot was created using correction liquid at each measurement location to provide a proper reflector. Adjacent to each spot, a PZT sensor was bonded to the surface of the pipe (see Figure 3). Figure 3 also depicts the arrangement of the measurement locations. The locations are numbered from 1, at the clamped end, to 5, at the free end. The same numbering was used for the PZTs.

To observe the free vibration of pipe, the pipe was excited with a piezoelectric impulse hammer (model 5800B5) manufactured by Dytran Instruments, Inc. The sensitivity of the hammer is 5 mV/lb and is able to apply a force up to 1000 lb. This hammer produces a constant force over the frequency range of interest. The output of the hammer is an analog voltage which is the representative of the input impulse.



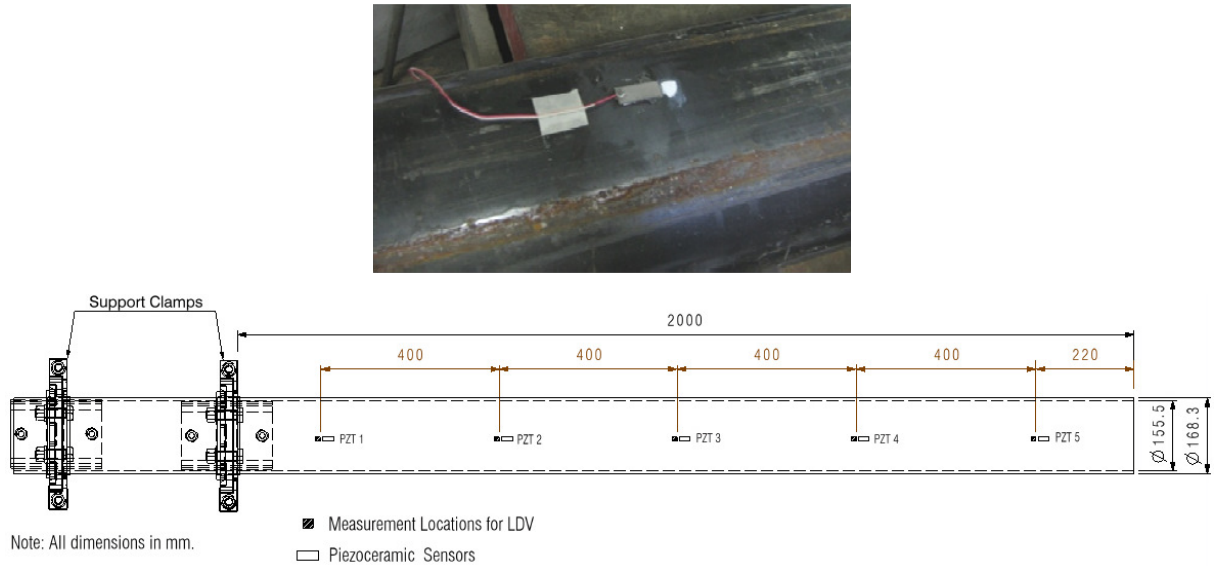


**Figure 3.** A typical reflective (white) spot and its adjacent PZT sensor on the pipe (top) and arrangement of measurement locations (bottom).

The impulse hammer can be equipped with either an aluminum tip or a hard plastic tip. The difference between the two tips is that the aluminum tip can excite frequencies up to 5 kHz while the hard plastic tip is only capable of exciting frequencies below 2 kHz. In the present study the aluminum tip was employed.

The responses of the LDV, impulse hammer, and PZT sensors were collected through a multifunction PCI-6220 data acquisition card manufactured by National Instruments, Inc. During all experiments the sampling frequency was kept at 20 kHz. The collected data was stored in an ASCII file which was then read by a MATLAB program, developed in-house, for processing. The code was constructed so that it could remove unwanted data before impact, compensate for any offset, normalize the signals, apply a band-pass filter, decompose the signals based on the EMD method, and finally calculate the energy of first IMF for each sensor. In order to remove the influence of the impact hammer on the pipe vibration, the acquired signals from sensors were normalized with respect to the hammer signal.

During the experiment, it was necessary to impact the free end of the pipe using the impulse hammer. It was observed that a slight change in the location of impact could affect the results. This change in location happened easily when the hammer was manually carried and guided to the impact location. To resolve this problem, a small steel ball (of diameter 12 mm) was glued to the free end of the pipe using Araldite 2011. This ball acted as a target for the impulse hammer thus ensuring impact at the same location on the pipe for each test. This method resulted in reasonable consistency for different impacts.

### Procedure of EMD damage detection

In order to employ the EMD damage detection methodology, the first step was to investigate the vibration of the pipe in its healthy state by using the LDV. Afterward, damage was introduced to the pipe and the vibration of the damaged pipe was monitored. The LDV responses from before and after the creation of

damage were processed by EMD, the energies of the first IMF for both the healthy and damaged states were calculated accordingly, and finally the EMD energy damage index (DI) was evaluated based on Equation (4). Once evaluated at each measurement location, the distribution of indices identified the location of damage on the pipe. The same procedure was employed for the PZT sensors and their results were compared with those of the LDV.

As stated earlier, the healthy pipe was restrained at one end by two clamps (see Figures 2 and 3). Clamp bolts were tightened to a torque of 145.0 Nm and the LDV beam was positioned to capture the vibration of the pipe at the measurement locations (the white spots in Figures 2 and 3). The LDV was set to a high velocity measurement setting with a low-pass filter of 5 kHz. After the pipe was impacted at the free end with the impulse hammer, the voltages of the impulse hammer and the LDV were acquired simultaneously by the data acquisition system. Following the collection of data for the first measurement location, the LDV was moved to the next location after which the pipe was again impacted and the LDV and hammer outputs were monitored. This procedure was repeated for all measurement locations to acquire the pipe vibration at all specified locations. After measurements were taken using the LDV, the pipe's vibrations were also monitored using the PZT sensors.

In order to achieve consistent results, the pipe was impacted three times for each measurement and the acquired signals were normalized based on the input force (the hammer signal). The difference between the signals after normalization was deemed to be a good measure of the repeatability of the impact procedure. To normalize the signals, the fast Fourier transform of each sensor response was divided by the fast Fourier transform of the hammer signal. The result was then transferred to time domain by the inverse fast Fourier transform. As mentioned above, the test was repeated three times for each case to ensure consistency of the results; their average was chosen as the EMD energy used in further calculations of the DI. Note that all these calculations were done by MATLAB code developed in-house.

The healthy pipe was then removed from the setup and damage was created by manually grinding the outer surface of the pipe. The damage was intended to simulate typical partial corrosion in a pipeline. Three damage cases were studied on the pipe. The first damage applied was material removal in the form of a half circumference with dimensions of 100 mm length and 3 mm depth, located halfway between measurement locations 3 and 4 (see Figure 4a). The second damage case extended the first damage to a full circumference with the same dimensions. In the third case, in addition to the first damage, another half-circumferential damage was created halfway between measurement locations 2 and 3 to represent multiple damages in the system (see Figure 4b). This damage had the same length and depth as in the first case. After creating the damage for each case, the pipe was placed in the setup and clamp bolts were tightened to the same torque as was used for the intact pipe. Subsequently the pipe was impacted and its free vibration was recorded by the data acquisition system. After collecting the response of the LDV at all measurement locations as well as the PZTs responses for the healthy and damaged pipe states, the developed MATLAB code was employed.

According to [Cheraghi and Taheri 2008], the acquired signal should be filtered through a band-pass so that the data will only contain the first natural frequency of the system. It was concluded that the suggested method works well for cases where the first frequency is the dominant vibrating frequency of the structure; otherwise, more frequency components should be included in the data to increase the accuracy of the proposed method. In the conducted experiment, the amplitude of the first frequency was of the same (or even lower) order as the other components (see Figure 5). Consequently, to improve

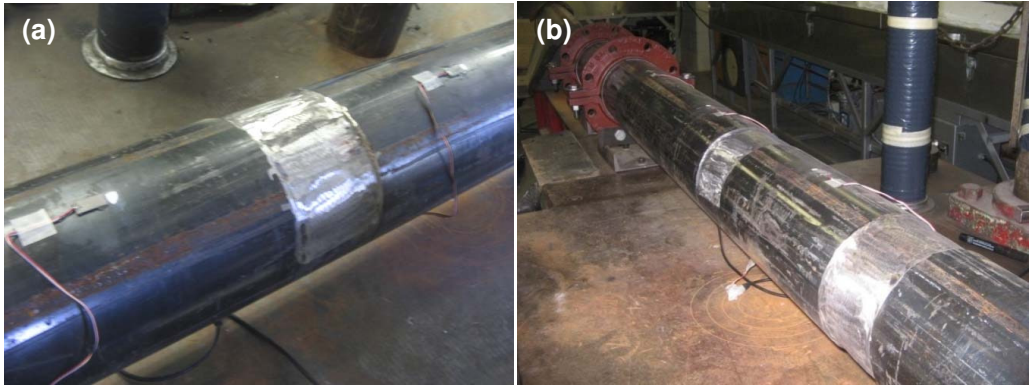


**Figure 4.** (a) Damage case 1: Half-circumferential damage between PZTs 3 and 4. (b) Damage case 3: Multiple damages—full-circumferential damage between PZTs 3 and 4 and half-circumferential damage between PZTs 2 and 3.

accuracy, a pass-band filter was designed in the MATLAB code to filter out all frequencies except the first six components. This filter was of the Butterworth type and passed frequencies in the range 10 Hz to 700 Hz.

The acquired signals from both the LDV and the PZT sensors lasted up to 3 s before decaying to zero. Considering the high sampling frequency used in the experiments, the acquired signal consisted of a huge amount of data, requiring lengthy processing time. Fortunately, the EMD energy DI is based on the comparison of special features in the PZT signals before and after the existence of damage; therefore, there are no limitations on the duration of the signals so long as the same duration is used for processing the pipe vibrations in the healthy and damaged states. Consequently, in the present work only the first 0.5 s of the signals were considered for evaluating the EMD energy.

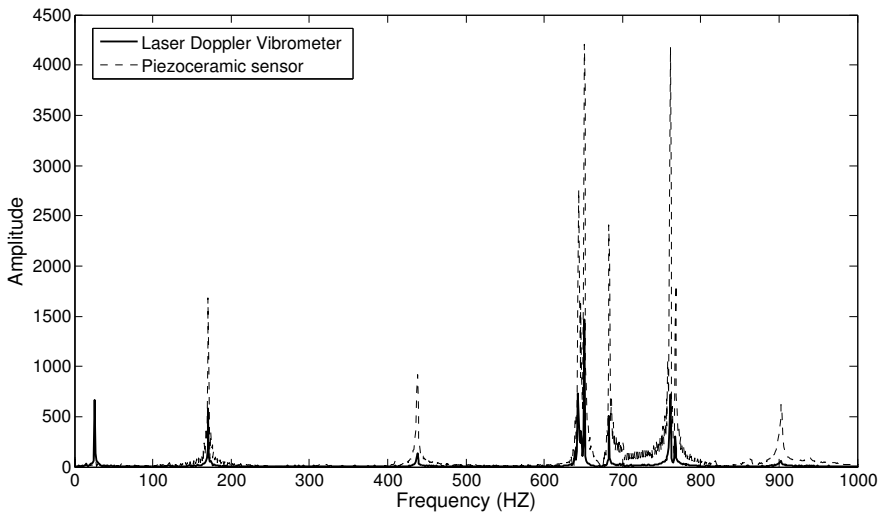


**Figure 5.** Frequency spectrum of response of the LDV at location 3 and its adjacent PZT.

### Results and discussion

Figure 5 illustrates the frequency spectrum obtained from the LDV at measurement location 3 and its adjacent PZT sensor. This figure shows a good agreement of the natural frequency extraction results between the LDV and the piezoceramic sensors. However, the LDV was not as successful as the PZT sensors in capturing all the frequencies. This can be explained by noting that the LDV is located on top of the pipe and can therefore only measure the flexural vibration modes in the vertical direction; it is unable to monitor in-plane vibrations. Consequently, those modes are missing in the frequency spectrum of the LDV.

Figure 6 illustrates a typical LDV response and its full decomposition via the EMD sifting process. The decomposition consists of seven IMF and a residue. As mentioned previously, the first IMF contains the highest frequency component within the data. Table 2 shows the energy of the first IMF of the LDV signals for the intact pipe at the five measurement locations. Table 3 lists the EMD energy for the first damage case. The EMD energy DI calculated from Equation (1) for the first damage case is illustrated using a bar chart in Figure 7. Figure 7 also shows a bar chart representing the EMD damage energy indices obtained from the piezoceramic sensors. Ignoring the DI at location 5 (PZT 5) it can be observed in both bar charts that the indices in the vicinity of the damage (locations 3 and 4, PZTs 3 and 4) are higher compared to those for locations 1 and 2. This clearly shows the capability of the proposed DI as well as the efficacy of the LDV in identifying and localizing the damage.

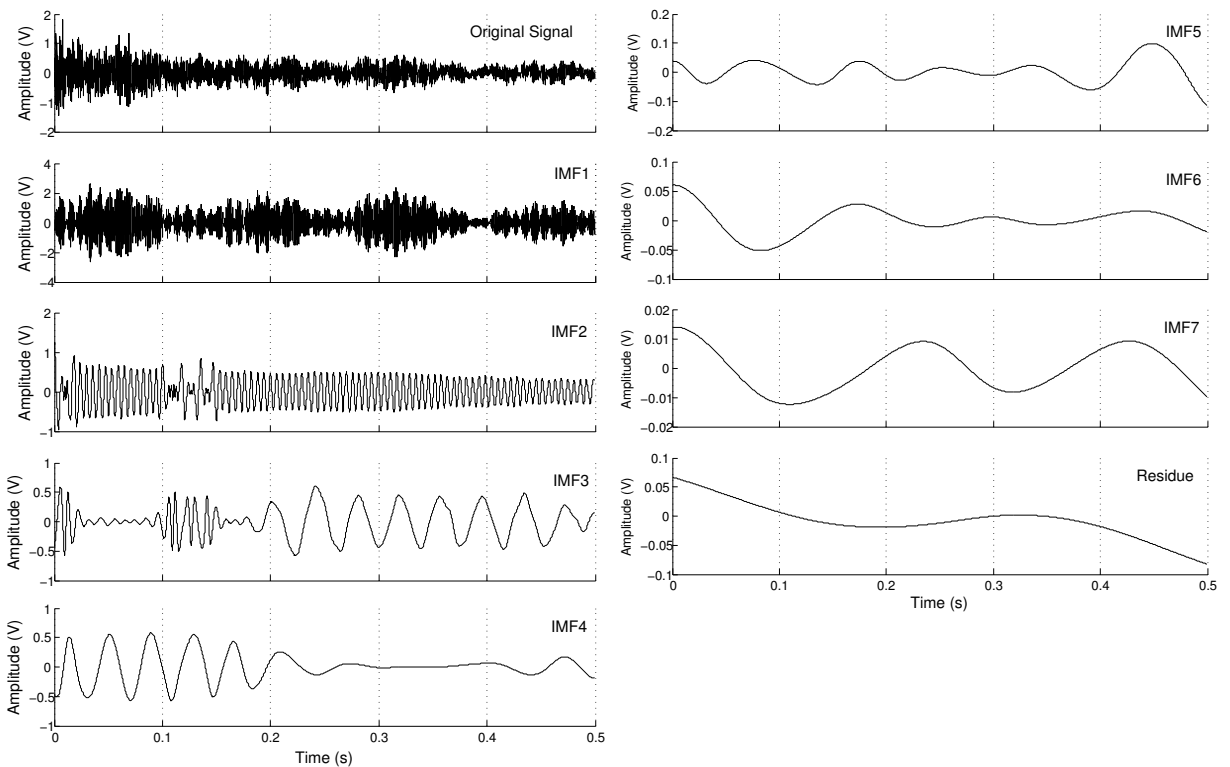


Figure 6. Typical PZT signal and its first five IMFs after decomposition.



|                          | Test 1   | Test 2   | Test 3   | Average  |
|--------------------------|----------|----------|----------|----------|
| LDV signal at location 1 | 0.169797 | 0.165133 | 0.181408 | 0.172112 |
| LDV signal at location 2 | 0.396397 | 0.454278 | 0.461394 | 0.437357 |
| LDV signal at location 3 | 0.345839 | 0.343561 | 0.371000 | 0.353467 |
| LDV signal at location 4 | 0.539827 | 0.484020 | 0.448339 | 0.490728 |
| LDV signal at location 5 | 0.560725 | 0.511886 | 0.546993 | 0.539868 |

**Table 2.** EMD energy of the first IMF of the pipe in its healthy state.

|                          | Test 1      | Test 2      | Test 3      | Average  |
|--------------------------|-------------|-------------|-------------|----------|
| LDV signal at location 1 | 0.155000041 | 0.143422832 | 0.139656454 | 0.146026 |
| LDV signal at location 2 | 0.415372962 | 0.36785452  | 0.346687328 | 0.376638 |
| LDV signal at location 3 | 0.181852193 | 0.186811528 | 0.214943954 | 0.194536 |
| LDV signal at location 4 | 0.135520932 | 0.135375133 | 0.139095011 | 0.136664 |
| LDV signal at location 5 | 0.957739222 | 0.8970118   | 0.971491258 | 0.942081 |

**Table 3.** EMD energy of the first IMF of the pipe in its damaged state (case 1: half-circumferential damage between locations 3 and 4).

The high value of the DI at location 5 (PZT 5) in [Figure 7](#), is due to the fact that this location is very close to the free end at which the pipe is impacted. Impact at that location produces considerable perturbations in the vibration in that vicinity and therefore the results from this sensor do not provide reliable results.

In [Figure 7](#), PZT 1 also has a relatively high DI value although there is no damage in the vicinity of this sensor. It is believed that this error was caused by the changes in the pipe's support conditions due to the removal of the pipe from its original setup state to create the damage, and then its replacement (which was unavoidable). It was practically impossible to reach the same boundary conditions as before the pipe removal even if the same torque was applied on the clamp bolts. Fortunately, this would not be encountered in real pipelines, since pipes are installed once and corrosion occurs gradually, and thus the support conditions remain the same. Interestingly, the LDV had smaller values at locations 1 and 5 (as

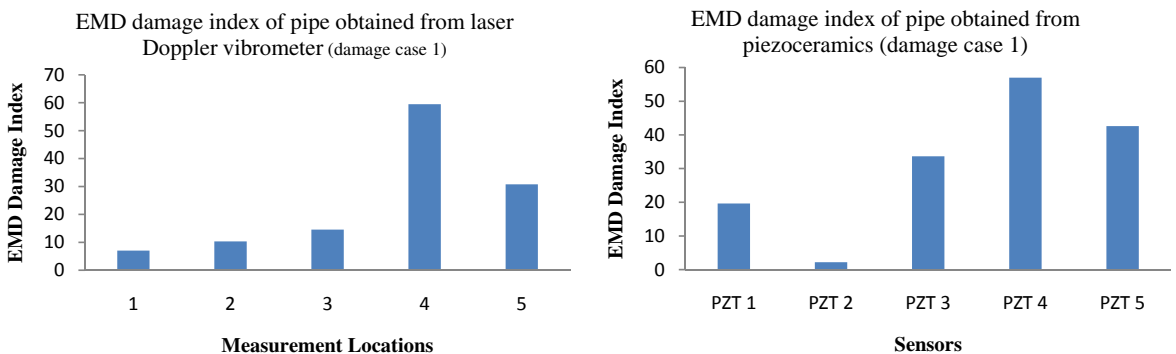


**Figure 7.** EMD damage index for the first damage case: a half circumference between locations 3 and 4.

opposed to PZTs 1 and 5). This shows that an advantage of the LDV over PZT sensors is less sensitivity to support conditions or impact location. A reason for this sensitivity reduction may be that the PZT sensors’ output is related to the longitudinal pipe while the LDV measures the pipe’s vertical vibrational velocity. Knowing this, it may be proposed that the boundary conditions and the impact location do not affect the velocity as much as the strain in the pipe. From Figure 7, it can be observed that the damage indices calculated from the LDV at locations 1 and 5 (where there was no damage) are lower than those obtained by the PZTs. The DI obtained from the LDV at location 4 (which is in the vicinity of the damage) is higher than that of PZT 4. However, the LDV predicted a lower DI at location 3 (which is in the vicinity of the damage) compared to the one calculated from PZT 3. Thus, in general it can be concluded that using the data obtained through LDV produced better damage identification compared to that taken through the piezoceramics.

Figure 8 depicts the EMD damage indices predicted by the LDV and the piezoceramics for the second damage case. The material removal for the second damage case was extended from the first case to a full circumference in order to examine more severe damage. Ignoring the signals from location 5, it can be seen that indices in the vicinity of the damage show higher values, which further demonstrates the applicability of the proposed damage methodology to locate damage. Comparing Figures 7 and 8, the following observations can be made:

- The damage indices computed from the LDV and PZTs at locations 3 and 4 for the second damage case are greater than those in the first case. This verifies the capability of the EMD DI in identifying the severity of damage.
- The LDV indices at locations 3 and 4 have higher values than those from the PZTs while at locations 1 and 5 the LDV indices are lower than those of the PZTs. This emphasizes the advantages of the LDV in terms of better damage location identification and less sensitivity to the boundary conditions and impact location.
- The damage indices obtained from the LDV show a greater difference between damage cases 1 and 2 compared to the PZT sensor results. This highlights the suitability of the LDV for damage severity assessment.

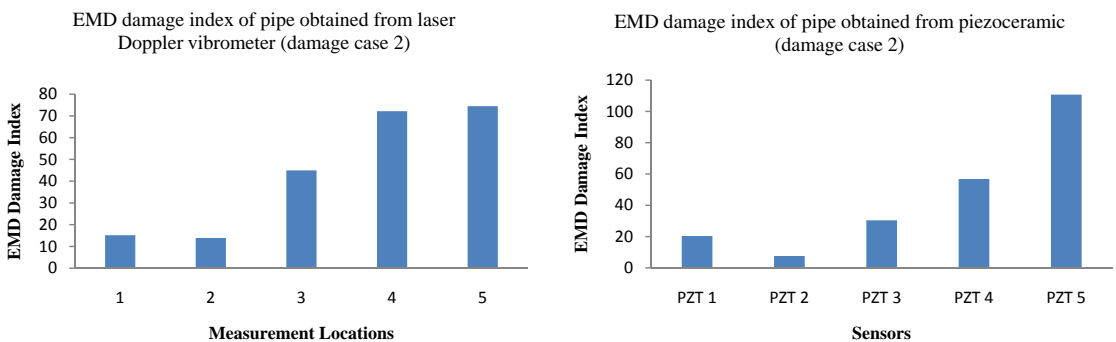
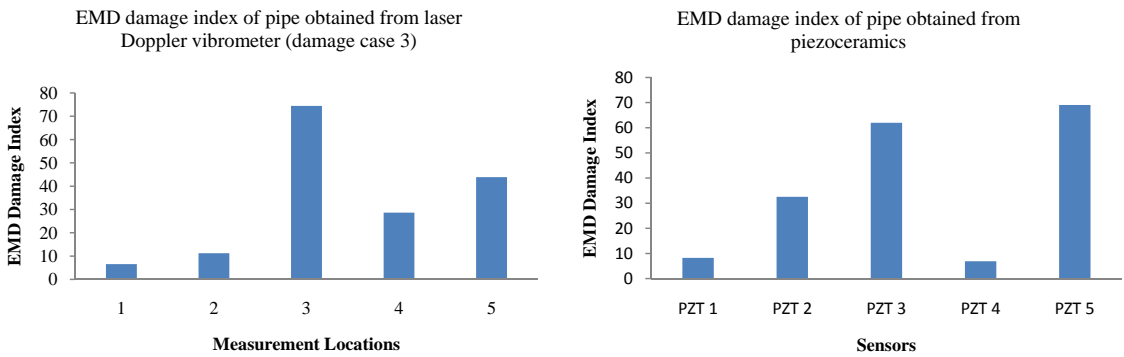


Figure 8. EMD damage index for the second damage case: a full circumference between locations 3 and 4.



**Figure 9.** EMD damage index for the third damage case: a full circumference between locations 3 and 4 and a half circumference between locations 2 and 3.

Based on these observations, use of the LDV provides a clearer damage identification method compared with use of the piezoceramic sensors.

The effectiveness of the EMD DI in detection of multiple damages is further illustrated in Figure 9 by considering the results of the LDV and piezoceramic sensors for the third damage case. In this case, a full-circumferential damage was created between locations 3 and 4 and a half-circumferential damage was created between locations 2 and 3. Neglecting the DI at location 5 (PZT 5), the bars in Figure 9 show higher indices at locations 2, 3, and 4, which are all in the vicinity of damages. This verifies the validity of the proposed methodology in identifying multiple damages. Moreover, the LDV has been shown to be an effective remote sensor that can be successfully utilized with an SHM methodology.

## Conclusion

In the present study, the applicability of the laser Doppler vibrometer (LDV) as a vibration measurement tool for structural health monitoring (SHM) was experimentally investigated through the application of a novel damage index (DI). This index is referred to as the EMD energy DI and is based on the Hilbert–Huang transform. For the experiment, a cantilever steel pipe was excited with an impulse hammer and its free vibrational velocity was acquired by the LDV at specified measurement locations. The vibration signals were then processed and decomposed via EMD and the energy of the first IMF for each signal was calculated for both the healthy and damaged pipe states. Three cases were analyzed to simulate various degrees of corrosion on the pipe surface: a single damage case (a partial circumference), a more severe single damage case (a full circumference), and a multiple damage case. In order to verify the LDV's results, they were compared with the results from PZT sensors bonded to the pipe's surface close to the LDV measurement locations.

The experimental results verified the capability of the LDV and the EMD energy DI to successfully detect and localize single and multiple damages in addition to qualifying damage severity. It was also observed that signal pass-band filtering should be carefully applied to avoid filtering out meaningful frequency components required for the proposed damage detection method. The frequency spectrum obtained from the LDV was in good agreement with the PZT results. However, a few frequency components were missing in the LDV results; these components corresponded to the in-plane vibration modes which the LDV was not able to capture. Compared to piezoceramic sensors, the LDV provided higher

damage indices at damage locations as well as a better assessment of damage severity. Furthermore, the LDV was less sensitive to boundary conditions and impact locations.

In general, use of the LDV as a remote and accurate high resolution optical measurement system provided satisfactory identification of single and multiple damages and can therefore be successfully utilized in SHM.

## References

- [API 2000] *API spec 5L: specification for line pipe*, 42nd ed., American Petroleum Institute, Washington, DC, 2000. Replaced by 44th edition.
- [Banks et al. 1996] H. T. Banks, D. J. Inman, D. J. Leo, and Y. Wang, “An experimentally validated damage detection theory in smart structures”, *J. Sound Vib.* **191**:5 (1996), 859–880.
- [Cheraghi and Taheri 2007] N. Cheraghi and F. Taheri, “A damage index for structural health monitoring based on the empirical mode decomposition”, *J. Mech. Mater. Struct.* **2**:1 (2007), 43–62.
- [Cheraghi and Taheri 2008] N. Cheraghi and F. Taheri, “Application of the empirical mode decomposition for system identification and structural health monitoring”, *Int. J. Appl. Math. Eng. Sci.* **2**:1 (2008), 61–72.
- [Cheraghi et al. 2005a] N. Cheraghi, M. J. Riley, and F. Taheri, “A novel approach for detection of damage in adhesively bonded joints in plastic pipes based on vibration method using piezoelectric sensors”, pp. 3472–3478 in *Proceedings of the International Conference on Systems, Man, and Cybernetics* (Waikoloa, HI, 2005), vol. 4, IEEE, Piscataway, NJ, 2005.
- [Cheraghi et al. 2005b] N. Cheraghi, G. P. Zou, and F. Taheri, “Piezoelectric-based degradation assessment of a pipe using Fourier and wavelet analyses”, *Comput.-Aided Civ. Infrastruct. Eng.* **20**:5 (2005), 369–382.
- [Douka et al. 2004] E. Douka, S. Loutridis, and A. Trochidis, “Crack identification in plates using wavelet analysis”, *J. Sound Vib.* **270**:1–2 (2004), 279–295.
- [Fukunaga et al. 2002] H. Fukunaga, N. Hu, and F.-K. Chang, “Structural damage identification using piezoelectric sensors”, *Int. J. Solids Struct.* **39**:2 (2002), 393–418.
- [Giurgiutiu et al. 2002] V. Giurgiutiu, A. Zagrai, and J. J. Bao, “Piezoelectric wafer embedded active sensors for aging aircraft structural health monitoring”, *Struct. Health Monit.* **1**:1 (2002), 41–61.
- [Hassiotis 2000] S. Hassiotis, “Identification of damage using natural frequencies and Markov parameters”, *Comput. Struct.* **74**:3 (2000), 365–373.
- [Hong et al. 2002] J.-C. Hong, Y. Y. Kim, H. C. Lee, and Y. W. Lee, “Damage detection using the Lipschitz exponent estimated by the wavelet transform: applications to vibration modes of a beam”, *Int. J. Solids Struct.* **39**:7 (2002), 1803–1816.
- [Huang et al. 1998] N. E. Huang, Z. Shen, S. R. Long, M. C. Wu, H. H. Shih, Q. Zheng, N.-C. Yen, C. C. Tung, and H. H. Liu, “The empirical mode decomposition and the Hilbert spectrum for nonlinear and non-stationary time series analysis”, *Proc. R. Soc. Lond. A* **454**:1971 (1998), 903–995.
- [Hwang and Kim 2004] H. Y. Hwang and C. Kim, “Damage detection in structures using a few frequency response measurements”, *J. Sound Vib.* **270**:1–2 (2004), 1–14.
- [Jian et al. 1997] X. H. Jian, H. S. Tzou, C. J. Lissenden, and L. S. Penn, “Damage detection by piezoelectric patches in a free vibration method”, *J. Compos. Mater.* **31**:4 (1997), 345–359.
- [Kaito et al. 2005] K. Kaito, M. Abe, and Y. Fujino, “Development of non-contact scanning vibration measurement system for real-scale structures”, *Struct. Infrastruct. Eng.* **1**:3 (2005), 189–205.
- [Khan et al. 2000] A. Z. Khan, A. B. Stanbridge, and D. J. Ewins, “Detecting damage in vibrating structures with a scanning LDV”, *Opt. Lasers Eng.* **32**:6 (2000), 583–592.
- [Kim and Chun 2004] H.-S. Kim and Y.-S. Chun, “Structural damage assessment of building structures using dynamic experimental data”, *Struct. Des. Tall Spec. Build.* **13**:1 (2004), 1–8.
- [Kim and Melhem 2004] H. Kim and H. Melhem, “Damage detection of structures by wavelet analysis”, *Eng. Struct.* **26**:3 (2004), 347–362.



- [Kim et al. 2003] J.-T. Kim, Y.-S. Ryu, H.-M. Cho, and N. Stubbs, “Damage identification in beam-type structures: frequency-based method vs. mode-shape-based method”, *Eng. Struct.* **25**:1 (2003), 57–67.
- [Lin et al. 2005] S. Lin, J. N. Yang, and L. Zhou, “Damage identification of a benchmark building for structural health monitoring”, *Smart Mater. Struct.* **14**:3 (2005), 162–169.
- [Liu et al. 2006] J. Liu, X. Wang, S. Yuan, and G. Li, “On Hilbert–Huang transform approach for structural health monitoring”, *J. Intell. Mater. Syst. Struct.* **17**:8–9 (2006), 721–728.
- [Nassif et al. 2005] H. H. Nassif, M. Gindy, and J. Davis, “Comparison of laser Doppler vibrometer with contact sensors for monitoring bridge deflection and vibration”, *NDT & E Int.* **38**:3 (2005), 213–218.
- [Ovanesova and Suarez 2004] A. V. Ovanesova and L. E. Suarez, “Applications of wavelet transforms to damage detection in frame structures”, *Eng. Struct.* **26**:1 (2004), 39–49.
- [Peeters et al. 1996] B. Peeters, M. Abdel Wahab, G. De Roeck, J. De Visscher, W. P. De Wilde, J.-M. Ndambi, and J. Vantomme, “Evaluation of structural damage by dynamic system identification”, pp. 1349–1361 in *Proceedings of ISMA21: 1996 International Conference on Noise and Vibration Engineering* (Leuven, 1996), edited by P. Sas, Katholieke Universiteit Leuven, Leuven, 1996.
- [Peeters et al. 2001] B. Peeters, J. Maeck, and G. De Roeck, “Vibration-based damage detection in civil engineering: excitation source and temperature effects”, *Smart Mater. Struct.* **10**:3 (2001), 518–527.
- [Polytec 2009] Polytec, “Single-point vibrometers”, 2009, Available at [http://www.polytec.com/usa/158\\_421.asp](http://www.polytec.com/usa/158_421.asp).
- [Ren and De Roeck 2002] W.-X. Ren and G. De Roeck, “Structural damage identification using modal data, II: Test verification”, *J. Struct. Eng. (ASCE)* **128**:1 (2002), 96–104.
- [Shi et al. 2000] Z. Y. Shi, S. S. Law, and L. M. Zhang, “Structural damage detection from modal strain energy change”, *J. Eng. Mech. (ASCE)* **126**:12 (2000), 1216–1223.
- [Soh et al. 2000] C. K. Soh, K. K.-H. Tseng, S. Bhalla, and A. Gupta, “Performance of smart piezoceramic patches in health monitoring of a RC bridge”, *Smart Mater. Struct.* **9**:4 (2000), 533–542.
- [Wang et al. 2001] X. Wang, N. Hu, H. Fukunaga, and Z. H. Yao, “Structural damage identification using static test data and changes in frequencies”, *Eng. Struct.* **23**:6 (2001), 610–621.
- [Winston et al. 2001] H. A. Winston, F. Sun, and B. S. Annigeri, “Structural health monitoring with piezoelectric active sensors”, *J. Eng. Gas Turb. Power (ASME)* **123**:2 (2001), 353–358.
- [Xu and Chen 2004] Y. L. Xu and J. Chen, “Structural damage detection using empirical mode decomposition: experimental investigation”, *J. Eng. Mech. (ASCE)* **130**:11 (2004), 1279–1288.

Received 27 Jan 2009. Revised 9 Jul 2009. Accepted 5 Aug 2009.

DAVOOD REZAEI: [drezaei@dal.ca](mailto:drezaei@dal.ca)

Department of Civil and Resource Engineering, Dalhousie University, 1360 Barrington St., Halifax, NS B3J 1Z1, Canada

FARID TAHERI: [farid.taheri@dal.ca](mailto:farid.taheri@dal.ca)

Department of Civil and Resource Engineering, Dalhousie University, 1360 Barrington St., Halifax, NS B3J 1Z1, Canada  
<http://myweb.dal.ca/farid/>

# JOURNAL OF MECHANICS OF MATERIALS AND STRUCTURES

<http://www.jomms.org>

Founded by Charles R. Steele and Marie-Louise Steele

## EDITORS

CHARLES R. STEELE Stanford University, U.S.A.  
DAVIDE BIGONI University of Trento, Italy  
IWONA JASIUK University of Illinois at Urbana-Champaign, U.S.A.  
YASUhide SHINDO Tohoku University, Japan

## EDITORIAL BOARD

H. D. BUI École Polytechnique, France  
J. P. CARTER University of Sydney, Australia  
R. M. CHRISTENSEN Stanford University, U.S.A.  
G. M. L. GLADWELL University of Waterloo, Canada  
D. H. HODGES Georgia Institute of Technology, U.S.A.  
J. HUTCHINSON Harvard University, U.S.A.  
C. HWU National Cheng Kung University, R.O. China  
B. L. KARIHALOO University of Wales, U.K.  
Y. Y. KIM Seoul National University, Republic of Korea  
Z. MROZ Academy of Science, Poland  
D. PAMPLONA Universidade Católica do Rio de Janeiro, Brazil  
M. B. RUBIN Technion, Haifa, Israel  
A. N. SHUPIKOV Ukrainian Academy of Sciences, Ukraine  
T. TARNAI University Budapest, Hungary  
F. Y. M. WAN University of California, Irvine, U.S.A.  
P. WRIGGERS Universität Hannover, Germany  
W. YANG Tsinghua University, P.R. China  
F. ZIEGLER Technische Universität Wien, Austria

## PRODUCTION

PAULO NEY DE SOUZA Production Manager  
SHEILA NEWBERY Senior Production Editor  
SILVIO LEVY Scientific Editor

Cover design: Alex Scorpan


Cover photo: Mando Gomez, [www.mandolux.com](http://www.mandolux.com)

See inside back cover or <http://www.jomms.org> for submission guidelines.

JoMMS (ISSN 1559-3959) is published in 10 issues a year. The subscription price for 2010 is US \$500/year for the electronic version, and \$660/year (+\$60 shipping outside the US) for print and electronic. Subscriptions, requests for back issues, and changes of address should be sent to Mathematical Sciences Publishers, Department of Mathematics, University of California, Berkeley, CA 94720-3840.

JoMMS peer-review and production is managed by EditFLOW™ from Mathematical Sciences Publishers.

PUBLISHED BY

 **mathematical sciences publishers**  
<http://www.mathscipub.org>

A NON-PROFIT CORPORATION

Typeset in L<sup>A</sup>T<sub>E</sub>X

©Copyright 2010. Journal of Mechanics of Materials and Structures. All rights reserved.

|  |            |
|--|------------|
| <b>A critical analysis of interface constitutive models for the simulation of delamination in composites and failure of adhesive bonds</b><br>ANTON MATZENMILLER, SEBASTIAN GERLACH and MARK FIOLKA          | <b>185</b> |
| <b>Computational studies of collagen fibril biominerals using a virtual internal bond model with extrinsic length scale</b><br>GANESH THIAGARAJAN and KAVITA DESHMUKH  | <b>213</b> |
| <b>The simulation of stochastically excited viscoelastic systems and their stability</b><br>VADIM D. POTAPOV   | <b>227</b> |
| <b>Fundamental solutions for an inhomogeneous cross-anisotropic material due to horizontal and vertical plane strain line loads</b><br>CHENG-DER WANG, JIA-YAN HOU and WEI-JER WANG                          | <b>241</b> |
| <b>Mechanical and fracture analysis of welded pearlitic rail steels</b><br>ALDINTON ALLIE, HESHMAT A. AGLAN and MAHMOOD FATEH  | <b>263</b> |
| <b>Rate dependence of indentation size effects in filled silicone rubber</b><br>RAMANJANEYULU V. S. TATIRAJU and CHUNG-SOUK HAN  | <b>277</b> |
| <b>A novel application of a laser Doppler vibrometer in a health monitoring system</b><br>DAVOOD REZAEI and FARID TAHERI   | <b>289</b> |
| <b>Energy absorption of a helicoidal bistable structure</b><br>SEUBPONG LEELAVANICHKUL, ANDREJ CHERKAEV, DANIEL O. ADAMS and FLORIAN SOLZBACHER  | <b>305</b> |
| <b>Decay properties of solutions of a Mindlin-type plate model for rhombic systems</b><br>FRANCESCA PASSARELLA, VINCENZO TIBULLO and VITTORIO ZAMPOLI  | <b>323</b> |
| <b>A consistent refinement of first-order shear deformation theory for laminated composite and sandwich plates using improved zigzag kinematics</b><br>ALEXANDER TESSLER, MARCO DI SCIUVA and MARCO GHERLONE | <b>341</b> |